Eur. Phys. J. B **11**, 643–654 (1999)

THE EUROPEAN PHYSICAL JOURNAL B

EDP Sciences

Interband collective electronic excitations in resonant Raman scattering of two-subband quantum wires

M. Sassetti[1], F. Napoli[1], and B. Kramer[2,a]

[1] Dipartimento di Fisica, INFM, Università di Genova, Via Dodecaneso 33, 16146 Genova, Italy
[2] I. Institut für Theoretische Physik, Universität Hamburg, Jungiusstraße 9, 20355 Hamburg, Germany

Received 8 February 1999

Abstract. Using the bosonization technique, a theory for the collective excitations of the interacting electrons in quantum wires with two subbands occupied is developed. The dispersion relations for the intersubband charge and spin density excitations are determined. The results are used to interpret the features observed in recent measurements of the Raman spectra of AlGaAs/GaAs quantum wires, particularly for photon energies near band gap resonance. It is shown that peaks previously identified as "single particle excitations" are signatures of higher order collective spin density excitations. Predictions about the observability of the interband modes are made.

PACS. 71.45.-d Collective effects – 78.30.-j Infrared and Raman spectra – 73.20.Dx Electron states in low-dimensional structures (superlattices, quantum well structures and multilayers)

1 Introduction

Recently, the low-temperature quantum mechanical properties of nano-structured semiconductor devices have become an important subject of condensed matter research [1]. Especially, the influence of the interaction on the electronic properties has been studied intensively experimentally and theoretically [2]. Raman scattering is one of the standard experimental methods to obtain insight into the nature of elementary excitations [3–8]. It has been applied extensively to semiconductor nano-structures.

Most strikingly, excitations have been found in both parallel and perpendicular polarizations of incoming and scattered light [9–14] when the energy of the incident photons approaches the energy of the gap between the valence and the conduction band. They violate the "classical selection rule", namely that (collective) charge and spin density excitations (CDE and SDE) are observed in parallel and perpendicular polarizations, respectively, and their energies correspond roughly to those of the pair excitations of the non-interacting electrons. Therefore, they have been associated with "single particle excitations" ("SPE"). However, this interpretation — at least for quantum wires — contradicts the well-known theoretical predictions which assert that there are solely *collective* low-energy excitations in the one dimensional (1D) interacting electron gas [15,16]. The experimentally detected energetically lowest excitations in quantum wires with only two subbands occupied are intraband CDE and SDE that are fully consistent with the theoretical predictions of the theory for 1D systems. This indicates that the interpretation of the polarization-insensitive features in the Raman spectra as "SPE" may be incorrect. Only by using the Bosonization method, which has been developed originally for the (1D) Luttinger liquid [17–19], some insight has been gained into the physical nature of these excitations [20–24]. It has been found that they can be related to higher-order spin density correlations which appear in the Raman spectra as peaks, but for the "wrong", namely parallel, relative polarization of incoming and scattered light.

In this paper, we provide the details of the previous calculations for two subbands. As the intraband excitations have been considered in detail earlier [21], we concentrate mainly on the extremely rich structure in the Raman spectra in the region of interband excitations when approaching resonance.

In the following Section 2 we describe qualitatively the collective excitations in quantum wires, review the experimental evidence and previous theoretical work, and summarize the present results. The model is described in Section 3. It can be used for the intra- as well as interband transitions. The Hamiltonian is diagonalized in Section 4, and the nature of the interband excitations is discussed. Section 5 contains the application to Raman scattering, Section 6 the comparison with the experiments and Section 7 the conclusion.

2 Collective modes in quantum wires

We start by considering the possible pair excitations of non-interacting electrons (effective mass m) that are confined within a quantum wire with only two occupied

[a] e-mail: kramer@physnet.uni-hamburg.de

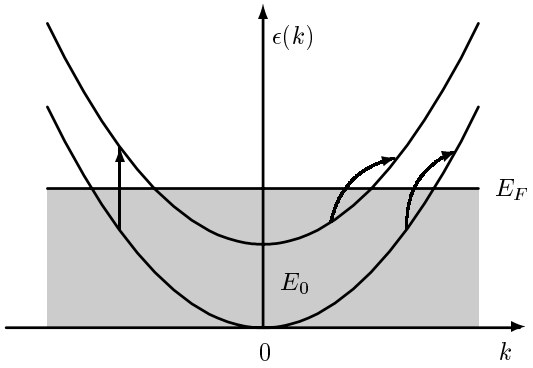

Fig. 1. One-electron subbands of a quantum wire with spacing E_0 and Fermi energy E_F such that two subbands are partially filled with particles. Arrows indicate possible pair excitations.

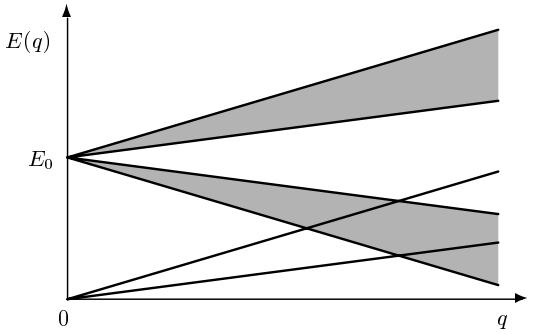

Fig. 2. Pair excitation energies of the non-interacting quasi-1D electron gas linearized for small wave numbers.

subbands (Fig. 1). Schematically, the excitation energies $E(q)$ are shown in Figure 2. For small wave number q and energy $E(q)$, they fulfill $|E(q) - \hbar v_{\mathrm{F}j} q| \leq \hbar^2 q^2/2m$ ($v_{\mathrm{F}j}$ Fermi velocity of subband j). For $q > 0$, there are no intraband excitations with small energies. This is the reason for the non-Fermi liquid behavior of the Luttinger liquid [18]. When the two lowest subbands are occupied, additional excitations become possible near $E(q) \approx E_0$ (E_0 subband spacing). They are restricted to $\hbar v_{\mathrm{F}2}|q| < |E(q) - E_0| < \hbar v_{\mathrm{F}1}|q|$, as long as the third subband is energetically far away. When the empty third band is separated from the second by about E_0, which is the case for the experimentally most important situation of parabolic confinement, pair excitations are also possible in the region $|E(q) - E_0| < \hbar v_{\mathrm{F}2}|q|$. Then, the common believe is that collective interband excitations cannot be expected to exist due to Landau damping. We will see below – by comparing with the experiments – that there is considerable evidence for the stability of collective excitations in this region.

For very small energies and $|q| \to 0$, only the collective CDE and SDE of the Luttinger liquid are expected to exist. However, as we will show below, for energies near E_0 one can define a model in analogy with the Luttinger liquid, which can be exactly diagonalized by using the bosonization method. *Stable collective excitations* will be shown to emerge. There is experimental evidence that these interband excitations do exist in quantum wires.

2.1 Status of experimental results

During the past decade, Raman scattering has been used to investigate in detail the elementary electronic excitations in quantum wires fabricated by laterally structuring the 2D electron gas in AlGaAs/GaAs heterostructures [9–14]. At small wave numbers, and excitation energies $E(q) = \hbar(\omega_{\mathrm{I}} - \omega_{\mathrm{O}}) \to 0$, intra-subband CDE and SDE have been found for photon energies well above the energy gap between valence and conduction band edges, with polarizations of incident (energy $\hbar\omega_{\mathrm{I}}$) and scattered (energy $\hbar\omega_{\mathrm{O}}$) photons parallel and perpendicular, respectively. By tracing the peak positions with wave number and excitation energy, the dispersion relations of CDE and SDE have been determined. The SDE was found to have linear dispersion, $\approx \hbar v_{\mathrm{F}1}|q|$, with $v_{\mathrm{F}1}$ the Fermi velocity of the lowest subband. The dispersion of the CDE was found to be renormalized by the interaction between the electrons and their energy approaches zero when $q \to 0$.

At higher energies, interband CDE and SDE have been found in wires with several subbands occupied. For $q \to 0$, the energies of these are non-zero, and represent the distances between the subbands, renormalized by interaction. Most of the data have been interpreted as being consistent with equidistant subbands, and this has been assumed to indicate parabolic confinement of the electrons. The position of the energetically lowest inter-subband CDE coincides approximately with E_0 [10], while the energy of the second lowest is considerably higher, roughly by a factor of two. This has been interpreted as indicating the presence of strong Coulomb repulsion in this mode [25].

In addition, when tuning the energies of the incident photons closer the band gap energy, new peaks appeared in the Raman spectra in parallel polarization. They violate the "classical selection rule" since they are also present in perpendicular polarization. The strengths of these peaks increase strongly, when the photon energy approaches the band gap. In the region of the intraband excitations, their dispersion laws were found to be approximately the same as those of the SDEs, almost not being influenced by the interaction. Consequently, these peaks have been associated with "SPE". They exist also for higher excitation energies, in the region of interband transitions, but their positions do not necessarily coincide exactly with those of the interband SDEs.

The properties of the intraband "SPE" have been investigated by using quantum wires with only two subbands occupied, the Fermi energy being situated just above the edge of the second subband [9,10]. In particular, it has been discussed, whether or not they could be interpreted as signature of an anti-symmetric combination of the charge density components corresponding to the two subbands. As this combination is expected to propagate with a velocity proportional to the square root of the Fermi velocities of the two subbands [15], the corresponding energy would become very small with the Fermi energy approaching the bottom of the second subband (Fig. 1). This is not consistent with the observations, as has been noted previously [9].

2.2 Previous theoretical work

The theory of the Raman spectra of quantum wires has been developed previously by using "classical" mean field approaches as the random phase approximation (RPA) [16,25]. The dispersion relation of the CDE in a one-subband quantum wire has been considered [16] using the leading-order dynamical screening approximation. The results have been found to be consistent with experiment as well as with the Tomonaga-Luttinger model [17,18] with Coulomb interaction [15]. The four possible CDEs in a two-subband quantum wire have been calculated by using a similar approach [25]. The dispersions of the two intraband CDEs are quite different. The symmetric CDE has a strongly non-linear dispersion which reflects the Fourier transform of the Coulomb interaction between the electrons. On the other hand, the dispersion of the anti-symmetric intraband CDE is linear, with a finite velocity of propagation. The two interband CDEs are again in-phase symmetric and out-of-phase anti-symmetric combinations of charge oscillations. The energy of the anti-symmetric mode has been found to coincide with E_0. The symmetric excitation is shifted to higher energy by the Coulomb repulsion (depolarization shift).

These results have been qualitatively confirmed by using the Hartree-Fock approximation [26,27]. There are, however, important quantitative differences, in addition to the possibility of treating the SDEs. The intraband out-of-phase CDE-mode is found to propagate with a velocity, which is proportional to the square root of the Fermi velocities corresponding to the two subbands, while the velocity of propagation of the intraband SDE of the energetically lowest subband is found to be slightly reduced by the exchange interaction. The inter-subband collective SDEs are again found to be only influenced by the exchange part of the interaction. Strong screening effects have been found when performing a self-consistent Hartree-Fock treatment of the many-subband case.

In these works, it has not been possible to address the problem of the "SPE" which appear in the *resonant* Raman spectra in both polarizations, since it has not been possible to calculate the Raman cross-section by using these approaches.

An approach which addresses this long-standing question has been developed recently by using the Tomonaga-Luttinger bosonization [15,17–19] for the intraband modes of a two-subband model [20,21,23]. This model allows not only to parametrize straightforwardly the dispersion relations of the four possible CDE- and SDE-modes in closed forms, but provides also insight into the physical nature of the previously unexplained "SPE"-features in the resonant Raman spectra. The reason is that the bosonization trick allows to calculate explicitly the Raman cross-section once the model is defined.

It has been found that the intraband "SPE" can be assigned to multiple SDE that contribute to the Raman spectra near resonance *via* higher order spin-correlation functions [20]. This explains in a natural way why the energetic positions of the intraband "SPE" coincide almost precisely with those of the intraband SDEs and does not depend on the position of the Fermi energy relative to the bottom of the second subband, as it was expected, if the intraband "SPE" was signature of the out-of-phase intraband CDE.

The bosonization method used for obtaining the intraband results has been generalized for treating interband excitations [24]. The first encouraging results indicate that also interband transitions can violate the "classical selection rule" when the photon energy approaches the energy gap, although the reasons are here more complex than in the case of the intraband transitions.

2.3 Summary of present results

In the present paper, we provide the details of a bosonization theory of Raman scattering on quantum wires with several subbands. We concentrate for the sake of simplicity on the energy region of the transitions between the two lowest subbands.

In order to be able to use the bosonization method for interband transitions, one has to decouple the intra- from the inter-subband modes. This can be achieved within a mean-field approximation which is described in detail in the next section. Once this is done, the Hamiltonian of the system becomes again essentially a quadratic form and the spectra of the intra- and inter-subband excitations as well as the Raman cross-sections can be calculated.

We find for the inter-subband modes – consistent with the above mentioned earlier results – two CDEs which are in-phase and out-of-phase combinations of interband charge densities and correspondingly two in-phase and out-of-phase SDE-modes. Only one of them, namely the in-phase CDE, is considerably influenced by the Coulomb repulsion which is shifted to higher energy in the limit of long wavelengths.

The intensities of the corresponding peaks in the Raman cross-section are also calculated, for both, off-resonance and near-resonance photon energies. For the lowest order processes, expressed in terms of single-pair density correlations, characteristic dependences of the intensities of the different CDE- and SDE-peaks as a function of the wave number are obtained. These may already account for some of the experimentally observed variations of the intensities. Taking into account higher order terms, more complicated combinations of charge and spin operators have to be considered and the "classical selection rule" is completely relaxed, as for the intraband transitions.

3 The model

In this section, we construct the Hamiltonian for quasi-1D confined interacting electrons with effective mass m. The one-particle spectrum consists of bands

$$\epsilon_j(k) = E_j + \frac{\hbar^2 k^2}{2m}, \tag{1}$$

where E_j $(j = 1, 2, 3, \dots)$ are the confinement energies. We assume that the Fermi energy $E_{\rm F}$ is such that two

subbands ($j = 1, 2$) are occupied with the corresponding Fermi wave numbers $k_{\mathrm{F}j} = \sqrt{2m(E_{\mathrm{F}} - E_j)}/\hbar$ and Fermi velocities $v_{\mathrm{F}j} = \hbar k_{\mathrm{F}j}/m$. The Hamiltonian of the non-interacting electrons is

$$H_0 = \sum_{j,s,k} \epsilon_j(k) c_{js}^\dagger(k) c_{js}(k), \tag{2}$$

with $c_{js}^\dagger(k)$, $c_{js}(k)$ the Fermion operators, $s = \pm$ denoting the spin quantum number and k the wave number.

3.1 Non-interacting electrons

For the collective excitations, it is useful to write H_0 as a quadratic form in the generalized density fluctuation operators

$$\rho_{ij,s}(q) = \sum_k c_{is}^\dagger(k+q) c_{js}(k)\,. \tag{3}$$

In order to bosonize the intraband excitations it has previously been found useful [18] to introduce new Fermion operators $c_{is}^{\lambda\dagger}(k)$, $c_{is}^{\lambda}(k)$ which correspond to independent branches $\mathrm{d}\epsilon(k)/\mathrm{d}k > 0$ ($k > 0$, $\lambda = +$) and $\mathrm{d}\epsilon(k)/\mathrm{d}k < 0$ ($k < 0$, $\lambda = -$) such that

$$\rho_{ij,s}(q) = \rho_{ij,s}^{+}(q) + \rho_{ij,s}^{-}(q)\,, \tag{4}$$

and to extend the Hilbert space of each of the branches to include the states with wave numbers of opposite sign, or, equivalently, states with negative energies. In analogy with the theory of the one-band Luttinger liquid, the charge fluctuations that couple different branches are defined with respect to the generalized average numbers of particles $n_{ij,s}^{\lambda}(k) \equiv \langle c_{is}^{\lambda\dagger}(k) c_{js}^{\lambda}(k)\rangle$

$$\rho_{ij,s}^{\lambda}(q) \equiv \sum_k \left(c_{is}^{\lambda\dagger}(k+q) c_{js}^{\lambda}(k) - n_{ij,s}^{\lambda}(k)\delta_{q,0} \right). \tag{5}$$

In view of the later inclusion of the interaction, the desired form of H_0 is a decomposition into independent parts, $H_0 = H_{\mathrm{intra}} + H_{\mathrm{inter}}$, which describe the intra- and inter-subband density fluctuations separately.

For diagonalizing the Hamiltonian in terms of collective pair excitations, it is necessary to construct commutation relations of the form

$$\left[H_0, \rho_{ij,s}^{\lambda}(q)\right] \propto \rho_{ij,s}^{\lambda}(q), \tag{6}$$

and

$$\left[\rho_{ij,s}^{\lambda}(q), \rho_{i'j',s'}^{\lambda'}(-q')\right] = \delta_{ss'}\delta_{\lambda\lambda'}\delta_{qq'}\delta_{ij'}\delta_{ji'}\frac{L}{2\pi}(k_{\mathrm{F}i} - k_{\mathrm{F}j} - \lambda\, q) \tag{7}$$

with the system length L.

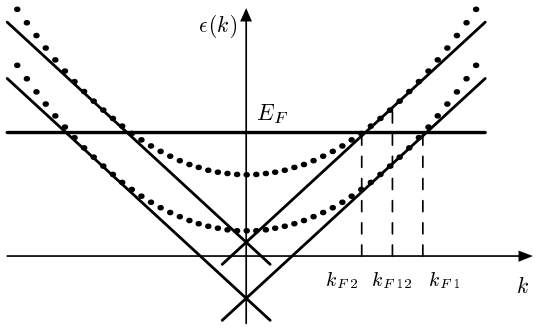

Fig. 3. The linear dispersion relations (full curves) assumed to treat the interband excitations, obtained from the two non-interacting electron bands (dotted curves) *via* the linearization around the mean Fermi wave number $k_{\mathrm{F}12}$.

By using (2, 3) one can show that

$$[H_0, \rho_{ij,s}(q)] = \left[E_i - E_j + \frac{\hbar^2 q^2}{2m}\right]\rho_{ij,s}(q) + \frac{\hbar^2 q}{m}\sum_k k c_{is}^\dagger(k+q) c_{js}(k)\,. \tag{8}$$

We note that the validity of (8) is guaranteed if it holds for each of the above branches separately. From the result in Appendix A, we obtain for the density fluctuations (with $v_{\mathrm{F}ij} \equiv (v_{\mathrm{F}i} + v_{\mathrm{F}j})/2$)

$$[H_0, \rho_{ij,s}^{\lambda}(q)] = [E_i - E_j + \hbar\lambda v_{\mathrm{F}ij} q]\,\rho_{ij,s}^{\lambda}(q) + \frac{\pi\lambda\hbar^2 q}{mL}\sum_{l=1,2}\sum_{q'}\rho_{ll,s}^{\lambda}(q-q')\rho_{ij,s}^{\lambda}(q'). \tag{9}$$

The second term on the right hand side describes an effective interaction between the pair excitations and creates multiple pairs. Decoupling of the modes can be achieved on the average by replacing ρ_{ll} by its average in the ground state, including the unphysical states with energies below zero. This average, however, vanishes as seen from (5), such that the desired form of the commutator is obtained. Similar approximations are standard in the mean-field theory of interacting systems [28]. The assumption is consistent with another one which we will use below to generate the commutation relations for the charge fluctuations.

For the intraband densities ρ_{ii} the above result corresponds to linearizing $\epsilon_i(k)$ around the Fermi wave numbers $\pm k_{\mathrm{F}i}$. On the other hand, for the interband densities ρ_{ij} ($i \neq j$), it corresponds to linearizing the two bands around the mean Fermi momentum $k_{\mathrm{F}ij} = m v_{\mathrm{F}ij}/\hbar$ (Fig. 3).

The commutators of the density fluctuations are

$$\left[\rho_{ij,s}^{\lambda}(q), \rho_{i'j',s'}^{\lambda'}(-q')\right] = \delta_{ss'}\delta_{\lambda\lambda'}\sum_k \Big[\delta_{ji'} c_{is}^{\lambda\dagger}(k+q-q') c_{j's}^{\lambda}(k) - \delta_{ij'} c_{i's}^{\lambda\dagger}(k-q') c_{js}^{\lambda}(k-q)\Big]\,. \tag{10}$$

By inserting (5) into (10) we find

$$\left[\rho^{\lambda}_{ij,s}(q),\rho^{\lambda}_{ji,s}(-q')\right]=\rho^{\lambda}_{ii,s}(q-q')-\rho^{\lambda}_{jj,s}(q-q') +\delta_{qq'}\sum_k\left(n^{\lambda}_{ii,s}(k)-n^{\lambda}_{jj,s}(k-q)\right). \quad (11)$$

In addition, there are mixed commutators between the intra- and the inter-subband densities

$$\left[\rho^{\lambda}_{ij,s}(q),\rho^{\lambda}_{i'i',s}(-q')\right]=\rho^{\lambda}_{ij,s}(q-q')(\delta_{ji'}-\delta_{ii'}) +\delta_{qq'}\sum_k\left(\delta_{ji'}n^{\lambda}_{ij,s}(k)-\delta_{ii'}n^{\lambda}_{ij,s}(k-q)\right). \quad (12)$$

The requested form of the intra-subband commutators are obtained from (12) for $i=j$,

$$\left[\rho^{\lambda}_{ii,s}(q),\rho^{\lambda'}_{i'i',s'}(-q')\right]=-\lambda q\frac{L}{2\pi}\delta_{ss'}\delta_{\lambda\lambda'}\delta_{ii'}\delta_{qq'}, \quad (13)$$

where we have used

$$\sum_k\left[n^{\lambda}_{ii,s}(k)-n^{\lambda}_{ii,s}(k-q)\right]=-\lambda\frac{Lq}{2\pi}\,. \quad (14)$$

For the interband commutators, the required form cannot exactly be derived, since both (11) and (12) are operators. However, with a mean field approximation similar to the one used above to decouple the equations of motion, we can define commutators which are of the required form. First, by taking the average of (12) for $i\neq j$ in a ground state which consists of products of one-particle states – for instance obtained by Hartree-Fock approximation – inter- and intra-subband density fluctuations become decoupled since both $\rho_{ij}(q)$ as well as $n_{ij}(q)$ vanish when averaged in such a state. Second, by averaging (11) and using again (14) we see that the right hand side gives

$$\delta_{qq'}\frac{L}{2\pi}\left(k_{\mathrm{F}i}-k_{\mathrm{F}j}-\lambda q\right).$$

Thus, for a model of a quantum wire with two (or more) subbands, the above (6) and (7) define a set of operators which can be used as a starting point for diagonalizing the many particle Hamiltonian with interaction.

In analogy with the RPA [25], we believe that our present mean field model incorporates the main physical mechanisms that are necessary to understand the fundamental collective electronic features of quantum wires in the region of the energies and wave numbers considered. In addition, the present model allows to calculate the Raman cross-section – even near resonance – because it can be bosonized. We are also able to extract by comparison with the experiments quantitative information about the electron-electron interaction and to predict features in the Raman spectra that have not yet been detected.

In summary, for describing the collective pair excitations of the interacting electrons, we start from the quadratic Hamiltonian of the non-interacting particles

$$H_0=\frac{\hbar\pi}{L}\sum_{i,j}v_{\mathrm{F}ij}\sum_{q,\lambda,s}\rho^{\lambda}_{ij,s}(q)\rho^{\lambda}_{ji,s}(-q). \quad (15)$$

3.2 The interaction matrix elements

For the interaction, we begin with the general form

$$\sum_{ss'}\sum_{ijlm}\sum_{qkk'}\hat{V}_{ijlm}(q)c^{\dagger}_{is}(k+q)c^{\dagger}_{js'}(k')c_{ls'}(k'+q)c_{ms}(k).$$

The matrix elements $\hat{V}_{ijlm}(q)$ are obtained by projecting a 3D screened Coulomb potential to the subbands and Fourier transforming with respect to the coordinate in the direction of the wire [21,25]. With the Fermion operators corresponding to left and right spectral branches one can decompose the interaction into many contributions.

As in H_0, inter- and intra-subband density fluctuations can be decoupled. The interaction matrix elements important for the intra-subband modes have been given previously [21]. We concentrate here on the matrix elements that are important for the interband modes,

$$\begin{aligned}H_{\mathrm{int}}=&\frac{1}{2L}\sum_q\sum_{\lambda\lambda'}\sum_{ss'}V_{12}(q)\left(\rho^{\lambda}_{12,s}(q)+\rho^{\lambda}_{21,s}(q)\right)\\&\times\left(\rho^{\lambda'}_{12,s'}(-q)+\rho^{\lambda'}_{21,s'}(-q)\right)\\&-\frac{1}{2L}\sum_{q,\lambda,s}V^{\mathrm{ex}}_{12}\left(\rho^{\lambda}_{12,s}(q)+\rho^{\lambda}_{21,s}(q)\right)\\&\times\left(\rho^{-\lambda}_{12,s}(-q)+\rho^{-\lambda}_{21,s}(-q)\right),\end{aligned} \quad (16)$$

where we have abbreviated

$$\begin{aligned}V_{12}(q)&=\hat{V}_{1122}(q)\\&=\hat{V}_{2211}(q)=\hat{V}_{1212}(q)=\hat{V}_{2121}(q),\end{aligned} \quad (17)$$

and

$$V^{\mathrm{ex}}_{12}=V_{12}(2k_{\mathrm{F}12}), \quad (18)$$

with $k_{\mathrm{F}12}=(k_{\mathrm{F}1}+k_{\mathrm{F}2})/2$.

In the Coulomb part of the interaction in (17), the back-scattering terms are omitted since we are not interested here in the subtleties that occur at zero temperature for $q\to 0$. There, the occurrence of a gap induced by back-scattering in some of the intraband modes, much smaller than the interband separation E_0, has been suggested [29–31]. For the interband modes at small but *non-zero* wave numbers (and $T\neq 0$) the back-scattering terms can be neglected. On the other hand, in the exchange part, only the back-scattering matrix elements are of importance. We assume here that (18) is the only non-vanishing contribution. This matrix element is, however, very small ($\approx 0.1V_{12}$), as seen by comparing the final results for the spectra with experiments (see below).

By introducing the charge and spin density operators

$$\begin{aligned}\rho^{\lambda}_{ij}(q)&=\frac{1}{\sqrt{2}}\left(\rho^{\lambda}_{ij,+}(q)+\rho^{\lambda}_{ij,-}(q)\right),\\\sigma^{\lambda}_{ij}(q)&=\frac{1}{\sqrt{2}}\left(\rho^{\lambda}_{ij,+}(q)-\rho^{\lambda}_{ij,-}(q)\right),\end{aligned} \quad (19)$$

one obtains that the CDE and SDE contribute independently, $H = H_\rho + H_\sigma$, with

$$H_\rho = \frac{h}{L} v_{\mathrm{F}12} \sum_{q,\lambda} \rho_{21}^{\lambda}(-q)\rho_{12}^{\lambda}(q) + \frac{1}{2L} \sum_{q,\lambda,\lambda'} [2V_{12}(q) + (\delta_{\lambda\lambda'} - 1)V_{12}^{\mathrm{ex}}] \times \left[(\rho_{12}^{\lambda}(q) + \rho_{21}^{\lambda}(q))(\rho_{12}^{\lambda'}(-q) + \rho_{21}^{\lambda'}(-q))\right], \quad (20)$$

$$H_\sigma = \frac{h}{L} v_{\mathrm{F}12} \sum_{q,\lambda} \sigma_{21}^{\lambda}(-q)\sigma_{12}^{\lambda}(q) - \frac{1}{2L} \sum_{q,\lambda} V_{12}^{\mathrm{ex}} \times \left[(\sigma_{12}^{\lambda}(q) + \sigma_{21}^{\lambda}(q))(\sigma_{12}^{\lambda'}(-q) + \sigma_{21}^{\lambda'}(-q))\right]. \quad (21)$$

Only the CDE are infuenced by the Coulomb repulsion. Since ρ_{12} commutes with σ_{12} the interband CDE- and SDE-energies may be determined by diagonalizing H_ρ and H_σ separately. From the definitions (19) one easily finds that the charge and the spin density operators fulfill the above commutation relations (7) separately.

4 Interband collective modes

In the following, we calculate eigenenergies and eigenvectors for the interband excitations with the method used by Penc and Solyom for the intraband modes [32].

4.1 Diagonalization

We first write the densities in terms of Bosons $a_\nu^\lambda(q)$

$$\nu_{12}^{\lambda}(q) = \sqrt{\varepsilon_0(1 - \lambda Q)}\, a_\nu^\lambda(q), \quad (22)$$

with $Q = \hbar v_{\mathrm{F}12} q / E_0 < 1$ and $\varepsilon_0 = L E_0 / h v_{\mathrm{F}12}$ ($\nu = \rho, \sigma$). The corresponding commutators are obtained from the commutators of the ν,

$$\left[a_\nu^\lambda(q), a_{\nu'}^{\lambda'\dagger}(q')\right] = \delta_{qq'}\delta_{\nu\nu'}\delta_{\lambda\lambda'}. \quad (23)$$

With these definitions, the Hamiltonians (20, 21) become

$$H_\nu = \sum_{q>0,i,j} \Psi_i^{(\nu)\dagger}(q) h_{ij}^{(\nu)}(q) \Psi_j^{(\nu)}(q), \quad (24)$$

with the vector operator

$$\Psi^{(\nu)\dagger}(q) \equiv \left(a_\nu^{+\dagger}(q), a_\nu^{-}(-q), a_\nu^{-\dagger}(q), a_\nu^{+}(-q)\right), \quad (25)$$

and its conjugate. The Hamiltonian matrix is

$$h^{(\nu)}(q) = E_0 \begin{pmatrix} h_- & b_- & c & d \\ b_- & h_- & d & c \\ c & d & h_+ & b_+ \\ d & c & b_+ & h_+ \end{pmatrix}, \quad (26)$$

$$\begin{aligned} h_\pm &= (1 + V\delta_{\nu\rho})(1 \pm Q) \\ b_\pm &= (V\delta_{\nu\rho} - V_{\mathrm{ex}})(1 \pm Q) \\ c &= (V\delta_{\nu\rho} - V_{\mathrm{ex}})(1 - Q^2)^{1/2} \\ d &= V\delta_{\nu\rho}(1 - Q^2)^{1/2} \end{aligned} \quad (27)$$

with the dimensionless interaction strengths

$$V = \frac{2V_{12}(q)}{h v_{\mathrm{F}12}}, V_{\mathrm{ex}} = \frac{V_{12}^{\mathrm{ex}}}{h v_{\mathrm{F}12}}. \quad (28)$$

The boson commutators in terms of (25) are

$$\left[\Psi_i^{(\nu)}(q), \Psi_j^{(\nu)\dagger}(q)\right] = \delta_{ij}(-1)^{(j+1)} \equiv D_{ij}. \quad (29)$$

We define new operators ($\alpha = 1 \ldots 4$)

$$\gamma_\alpha^{(\nu)}(q) = \sum_j w_{\alpha j}^{(\nu)}(q) \Psi_j^{(\nu)}(q), \quad (30)$$

with the real coefficients $w_{\alpha j}^{(\nu)}(q)$ chosen such that $\gamma^{(\nu)}$ diagonalize the Hamiltonians,

$$\left[H_\nu, \gamma_\alpha^{(\nu)}(q)\right] = -\hbar\omega_\alpha^{(\nu)}(q)\gamma_\alpha^{(\nu)}(q). \quad (31)$$

By inserting (30) into (31) we get

$$\sum_{l,j} h_{il}^{(\nu)}(q) D_{lj} w_{\alpha j}^{(\nu)}(q) = \hbar\omega_\alpha^{(\nu)}(q) w_{\alpha i}^{(\nu)}(q). \quad (32)$$

The eigenvalues are determined by the quartic equation

$$\det\left[\sum_l h_{il}^{(\nu)}(q) D_{lj} - \hbar\omega_\alpha^{(\nu)}(q)\delta_{ij}\right] = 0. \quad (33)$$

This does not yield directly the eigenvalues of H_ν which are expected to be positive. Instead, $\hbar\omega_\alpha^{(\nu)}(q)$ are the eigenvalues of $H_\nu D$. It is, however, possible to obtain the eigenvalues of H from those of $H_\nu D$. For this, we need to evaluate the commutators of the γ-operators,

$$\left[\gamma_\alpha^{(\nu)}(q), \gamma_\beta^{(\nu)\dagger}(q)\right] = \sum_{i,j} w_{\alpha i}^{(\nu)}(q) D_{ij} w_{\beta j}^{(\nu)}(q), \quad (34)$$

which is generally not $\delta_{\alpha\beta}$, because D is not positive definite. In order to obtain the eigenvalues of H, we assume [32]

$$\sum_{i,j} w_{\alpha i}^{(\nu)}(q) D_{ij} w_{\beta j}^{(\nu)}(q) = \delta_{\alpha\beta}\mathrm{sgn}(\omega_\alpha^{(\nu)}(q)). \quad (35)$$

We write the Hamiltonian in terms of the eigenmodes $\gamma_\alpha^{(\nu)}$ by inserting the inverse of (30), which is obtained by using (35),

$$\Psi_i^{(\nu)}(q) = \sum_{\alpha,j} \mathrm{sgn}(\omega_\alpha^{(\nu)}(q)) D_{ij} w_{\alpha j}^{(\nu)}(q) \gamma_\alpha^{(\nu)}(q), \quad (36)$$

into (24),

$$H_\nu = \sum_{q>0,\alpha} E_\alpha^{(\nu)}(q)\gamma_\alpha^{(\nu)\dagger}(q)\gamma_\alpha^{(\nu)}(q) \tag{37}$$

with the positive eigenenergies

$$E_\alpha^{(\nu)}(q) \equiv \hbar\omega_\alpha^{(\nu)}(q)\mathrm{sgn}(\omega_\alpha^{(\nu)}(q)), \tag{38}$$

but corresponding to the non-bosonic eigenmodes (34).

The secular equation (33) is bi-quadratic. Therefore, its eigenvalues come in pairs and $E_\alpha^{(\nu)}(q)$, which are so far defined only for $q > 0$, are twofold degenerate. The index α is chosen in such a way that $E_1^{(\nu)} = E_3^{(\nu)}$ and $E_2^{(\nu)} = E_4^{(\nu)}$. By suitably re-defining the γ-operators (Appendix B), the degeneracy is lifted such that one set of the $E_\alpha^{(\nu)}(q)$ corresponds to $q < 0$. The re-definition simultaneously creates bosonic creation and annihilation operators from the γ-operators.

4.2 Eigenenergies

The eigenvalue equation for $H_\nu D$ (33) can be solved analytically. The results are given in Appendix B. In Figure 4 we show both pairs of solutions for H_ρ (CDE) and H_σ (SDE), $E_\alpha^{(\rho,\sigma)}(q)$ ($\alpha = 1, 2$) for $V(q \to 0)$. For small q we have

$$\frac{E_\alpha^{(\nu)}(q)}{E_\alpha^{(\nu)}(0)} \approx \left(1 + (-1)^{\alpha+1} A_\alpha^{(\nu)} \frac{\hbar^2 q^2 v_{\mathrm{F}12}^2}{2\left[E_\alpha^{(\nu)}(0)\right]^2}\right), \tag{39}$$

where the energy values at $q = 0$ are

$$\frac{E_\alpha^{(\rho)}(0)}{E_0} = \sqrt{1 + 2(1 + (-1)^{\alpha+1})V + 2(-1)^\alpha V_{\mathrm{ex}}} \tag{40}$$

$$\frac{E_\alpha^{(\sigma)}(0)}{E_0} = \sqrt{1 + 2(-1)^\alpha V_{\mathrm{ex}}}, \tag{41}$$

and the curvatures to $\mathrm{O}(V_{\mathrm{ex}})$

$$A_\alpha^{(\rho)} = \frac{1 + (4 + (-1)^{\alpha+1})V + 2(1 + (-1)^{\alpha+1})V^2}{V} \tag{42}$$

$$A_\alpha^{(\sigma)} = -\frac{1}{V_{\mathrm{ex}}}. \tag{43}$$

4.3 Eigenmodes

The eigenmodes corresponding to the above energies are obtained from (32). They fulfill the relations

$$\sum_{j=1}^{4} [w_{\alpha j}^{(\nu)}(q)]^2 (-1)^{j+1} = \mathrm{sgn}\left(\omega_\alpha^{(\nu)}(q)\right), \tag{44}$$

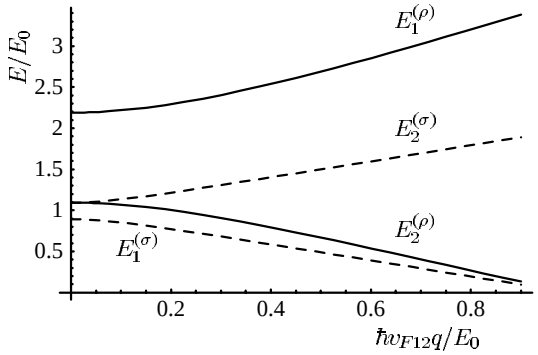

Fig. 4. Excitation energies E of CDE (full lines) and SDE (dashed) as a function of the wave number q ($V = 1.0$, $V_{\mathrm{ex}} = 0.1$, E_0 inter-subband distance, $v_{\mathrm{F}12}$ average Fermi velocity).

(the normalization condition (35))

$$\frac{w_{\alpha 2}^{(\nu)}(q)}{w_{\alpha 1}^{(\nu)}(q)} = K_\alpha^{(\nu)}(q)\frac{\hbar\omega_\alpha^{(\nu)}(q) - E_0(1+Q)}{\hbar\omega_\alpha^{(\nu)}(q) + E_0(1-Q)}, \tag{45}$$

$$\frac{w_{\alpha 3}^{(\nu)}(q)}{w_{\alpha 1}^{(\nu)}(q)} = K_\alpha^{(\nu)}(q)\sqrt{\frac{1+Q}{1-Q}}, \tag{46}$$

and

$$\frac{w_{\alpha 4}^{(\nu)}(q)}{w_{\alpha 1}^{(\nu)}(q)} = \frac{\hbar\omega_\alpha^{(\nu)}(q) - E_0(1-Q)}{\hbar\omega_\alpha^{(\nu)}(q) + E_0(1+Q)}\sqrt{\frac{1+Q}{1-Q}}\,. \tag{47}$$

The factor $K_\alpha^{(\nu)}(q)$ is given in Appendix B. These relations can be manipulated to provide the final results that are needed, in order to evaluate the Raman cross-sections. The expressions for $w_{\alpha 1}^{(\nu)}(q)$, which are eventually needed, are given in Appendix B.

5 The Raman spectrum

5.1 The differential cross-section

Within the theory of Raman scattering [3–5] the differential cross-section is given by

$$\frac{\mathrm{d}\sigma}{\mathrm{d}\Omega\mathrm{d}\omega} = \left(\frac{e^2}{m_0 c^2}\right)^2 \frac{\omega_{\mathrm{O}}}{\omega_{\mathrm{I}}}\frac{n(\omega)+1}{\pi}\mathcal{I}\mathrm{m}\chi(\mathbf{q},\omega), \tag{48}$$

where I and O denote initial and final states, respectively, $\omega = \omega_{\mathrm{I}} - \omega_{\mathrm{O}}$ the difference between the frequencies of the incident and the scattered light, respectively, $\mathbf{q} = \mathbf{k}_{\mathrm{I}} - \mathbf{k}_{\mathrm{O}}$ the wave vector transfer, m_0 the bare electron mass and $n(\omega)$ the Bose distribution.

The correlation function

$$\chi(\mathbf{q},t) = \mathrm{i}\Theta(t)\langle\left[N^\dagger(\mathbf{q},t), N(\mathbf{q},0)\right]\rangle, \tag{49}$$

is expressed in terms of the generalized density operator

$$N(\mathbf{q}) = \sum_{\alpha,\alpha'} \Gamma_{\alpha,\alpha'}(\mathbf{k}_{\mathrm{I}}, \mathbf{k}_{\mathrm{F}}) c_\alpha^\dagger c_{\alpha'}. \tag{50}$$

It contains the creation and annihilation operators of the electrons in the conduction band states $|\alpha\rangle$, $|\alpha'\rangle$, and the transition matrix elements $\Gamma_{\alpha,\alpha'}$ between valence and conduction electrons due to the electromagnetic field. These contain terms proportional to $\mathbf{A}^2$ and $\boldsymbol{\Pi}\cdot\mathbf{A}$ ($\mathbf{A}$ vector potential of the light, $\boldsymbol{\Pi}$ momentum operator, respectively). The latter term is treated in second order, in order to be consistent. The evaluation of the matrix elements requires further approximations, especially near resonance.

5.2 Generalized densities and interband modes

Assuming the quasi-1D geometry described in Section 3, and neglecting both anisotropy and non-parabolicity effects we can write [21]

$$N(q) = \sum_{i\neq j,ss',\lambda} \sum_{k} \frac{\Gamma_{is,js'}}{D_i(k,q)} c_{is}^{\lambda\dagger}(k+q) c_{js'}^{\lambda}(k), \qquad (51)$$

where the summation over the band indices is restricted to $i \neq j$ and $i,j = 1,2$, because we consider here only the interband excitations between the subbands 1 and 2. The wave number q is the component of $\mathbf{q}$ along the wire. The matrix elements $\Gamma_{is,js'}$ can be written as [21]

$$\Gamma_{is,js'} = \delta_{ss'}\left[\Gamma^{(1)}\mathbf{e}_{\rm O}\cdot\mathbf{e}_{\rm I} + \mathrm{i}\Gamma^{(2)} s|\mathbf{e}_{\rm I}\times\mathbf{e}_{\rm O}|\right], \qquad (52)$$

with the constants $\Gamma^{(1,2)}$ representing average transition matrix elements. The energy denominator $D_i(k,q)$ is

$$D_i(k,q) = E_{\rm G}^0 + E_i - \hbar\omega_{\rm I} + \frac{\hbar^2}{2m}(k+q)^2, \qquad (53)$$

where we assumed a dispersionless valence band, and $E_{\rm G}^0$ is the energy difference between the top of valence band and the bottom of the bulk conduction band.

In order to perform the sum over k, we expand the quantity $D_i(k,q)^{-1}$ into a power series

$$\frac{1}{D_i(k,q)} = \sum_{n=0}^{\infty} \frac{[-X_\lambda(k)]^n}{\left(E_{\rm G} + E_i - \hbar\omega_{\rm I} + \lambda\hbar v_{\rm F12} q/2\right)^{(n+1)}} \qquad (54)$$

where

$$E_{\rm G} = E_{\rm G}^0 + \frac{\hbar^2 k_{\rm F12}^2}{2m} + \frac{\hbar^2 q^2}{8m}, \qquad (55)$$

$$X_\lambda(k) = \frac{\hbar^2\kappa_\lambda^2(k,q)}{2m} + \frac{\hbar^2}{m}\kappa_\lambda(k,q)\left(\lambda k_{\rm F12} + \frac{q}{2}\right) \qquad (56)$$

with

$$\kappa_\lambda(k,q) = k - \lambda k_{\rm F12} + \frac{q}{2}\cdot \qquad (57)$$

We show in Appendix A that, with the boson representation of the fermions c and $c^\dagger$, the n-th term ($n > 1$) of the expansion can be written as a product of the interband densities with $n-1$ intraband density modes. These higher-order terms lead to a breakdown of the "classical selection rule" such that structure related to SDE can appear in the polarized configuration, and CDE-related features in the depolarized configuration. However, as discussed below, the only peak-like structure appears in the polarized spectra and is due to the SDE.

Neglecting for the moment the higher order contributions and summing over the spin variable, we have ($\Delta_i = E_{\rm G} + E_i - \hbar\omega_{\rm I}$)

$$N^{(0)}(q) = \sum_{i\neq j,\lambda} \frac{\sqrt{2}}{\Delta_i + \lambda\hbar v_{\rm F12} q/2} \times \left[\Gamma^{(1)}\mathbf{e}_{\rm I}\cdot\mathbf{e}_{\rm O}\rho_{ij}^{\lambda}(q) + \mathrm{i}\Gamma^{(2)}|\mathbf{e}_{\rm I}\times\mathbf{e}_{\rm O}|\sigma_{ij}^{\lambda}(q)\right]. \qquad (58)$$

This shows that CDE and SDE can be seen only in the polarized and the depolarized configuration, respectively.

Summing over the branches λ, we get

$$N^{(0)}(q) = \sum_{i\neq j} \frac{1}{\Delta_i^2 - \hbar^2 v_{\rm F12}^2 q^2/4} \times \left\{\Gamma^{(1)}\mathbf{e}_{\rm I}\cdot\mathbf{e}_{\rm O}\left[2\Delta_i\rho_{ij}^s(q) - \hbar v_{\rm F12} q\rho_{ij}^a(q)\right] + \mathrm{i}\Gamma^{(2)}|\mathbf{e}_{\rm I}\times\mathbf{e}_{\rm O}|\left[2\Delta_i\sigma_{ij}^s(q) - \hbar v_{\rm F12} q\sigma_{ij}^a(q)\right]\right\}, \qquad (59)$$

where we have introduced symmetric and anti-symmetric combinations of left- and right-moving branches,

$$\nu_{ij}^s(q) = \frac{1}{\sqrt{2}}\left(\nu_{ij}^+(q) + \nu_{ij}^-(q)\right), \qquad (60)$$

$$\nu_{ij}^a(q) = \frac{1}{\sqrt{2}}\left(\nu_{ij}^+(q) - \nu_{ij}^-(q)\right). \qquad (61)$$

For the evaluation of the Raman cross-section, we express these in terms of the eigenmodes,

$$\nu_{12}^{s,a}(q) = \sqrt{\frac{\varepsilon_0}{2}}\sum_{\alpha=1}^{4} \mathrm{sgn}(\omega_\alpha^{(\nu)}(q))\gamma_\alpha^{(\nu)}(q) \times \left[w_{\alpha1}^{(\nu)}(q)\sqrt{1-Q} \pm w_{\alpha3}^{(\nu)}(q)\sqrt{1+Q}\right], \qquad (62)$$

$$\nu_{21}^{s,a}(q) = -\sqrt{\frac{\varepsilon_0}{2}}\sum_{\alpha=1}^{4} \mathrm{sgn}(\omega_\alpha^{(\nu)}(q))\gamma_\alpha^{(\nu)}(q) \times \left[w_{\alpha4}^{(\nu)}(q)\sqrt{1+Q} \pm w_{\alpha2}^{(\nu)}(q)\sqrt{1-Q}\right]. \qquad (63)$$

On the right hand side, $\pm$ correspond to the symmetric and the anti-symmetric combinations, respectively.

5.3 Off resonance

When the frequency of the incoming light is much higher than that corresponding to the energy gap,

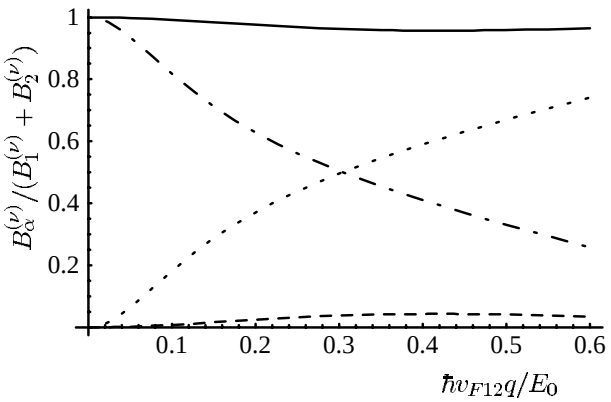

Fig. 5. Intensities of peaks $B_\alpha^{(\nu)}/(B_1^{(\nu)}+B_2^{(\nu)})$ off-resonance as a function of the wave number q ($V=1$, $V_{\rm ex}=0.1$). Full line: $B_1^{(\rho)}$; dashed: $B_2^{(\rho)}$; dashed-dotted: $B_1^{(\sigma)}$; dotted: $B_2^{(\sigma)}$.

$|E_{\rm G}-\hbar\omega_{\rm I}| \gg E_i > \hbar v_{\rm F12} q/2$, we get from (59)

$$N^{(0)}(q) = \frac{2}{E_{\rm G}-\hbar\omega_{\rm I}} \left[\Gamma^{(1)}\, \mathbf{e}_{\rm I}\cdot\mathbf{e}_{\rm O} \sum_{i\neq j} \rho_{ij}^{s}(q) + {\rm i}\Gamma^{(2)} |\mathbf{e}_{\rm I}\times\mathbf{e}_{\rm O}| \sum_{i\neq j} \sigma_{ij}^{s}(q) \right]. \quad (64)$$

With this, we obtain the correlation function ($\omega>0$)

$$\mathcal{I}{\rm m}\chi(q,\omega) = \frac{4\pi\hbar}{(E_{\rm G}-\hbar\omega_{\rm I})^2} \times \left\{ \left(\Gamma^{(1)}\mathbf{e}_{\rm I}\cdot\mathbf{e}_{\rm O}\right)^2 \sum_{\alpha=1,2} B_\alpha^{(\rho)}(q)\delta(\hbar\omega - E_\alpha^{(\rho)}(q)) + \left(\Gamma^{(2)}|\mathbf{e}_{\rm I}\times\mathbf{e}_{\rm O}|\right)^2 \sum_{\alpha=1,2} B_\alpha^{(\sigma)}(q)\delta(\hbar\omega - E_\alpha^{(\sigma)}(q)) \right\}. \quad (65)$$

The intensities $B_\alpha^{(\nu)}(q)$ are obtained from (62) and (63)

$$B_\alpha^{(\nu)}(q) = \varepsilon_0 \left[\sqrt{1-Q}\left(w_{\alpha1}^{(\nu)}(q) - w_{\alpha2}^{(\nu)}(q)\right) + \sqrt{1+Q}\left(w_{\alpha3}^{(\nu)}(q) - w_{\alpha4}^{(\nu)}(q)\right)\right]^2. \quad (66)$$

Figure 5 shows the dependence of the peak intensities of the interband CDE and SDE on the wave number. In the polarized spectrum, the energetically highest CDE at energy $E_1^{(\rho)}$ carries almost all of the weight, while the CDE mode at the lower energy $E_2^{(\rho)}$ is almost completely suppressed. In the depolarized configuration, there is a cross-over between the modes: for small wave vector, the energetically higher SDE at $E_2^{(\sigma)}$ is suppressed in favor of the energetically lower one at $E_1^{(\sigma)}$. This is reversed for larger q.

5.4 Near resonance

When the energy of the incoming photons approaches $E_{\rm G}+E_i$, the dependence of the denominator $D_i(k,q)$ on the wave number has to be taken into account. For the interband excitations, there are two contributions. One is due to $N^{(0)}(q)$, the other originates in the higher-order terms of (54).

The contribution due to $N^{(0)}(q)$ is obtained from (59) in the extreme limit $\Delta_i < \hbar^2 v_{\rm F12} q/2$. We consider $i=2$. The corresponding $N^{(0)}(q)$ is analogous to (64) but contains ρ^a instead of ρ^s. We find for the correlation function

$$\mathcal{I}{\rm m}\chi(q,\omega) = 4\pi\hbar \left[\frac{\hbar v_{\rm F12} q}{\Delta_2^2 - \hbar^2 v_{\rm F12}^2 q^2/4}\right]^2 \times \left\{ \left(\Gamma^{(1)}\mathbf{e}_{\rm I}\cdot\mathbf{e}_{\rm O}\right)^2 \sum_{\alpha=1,2} C_\alpha^{(\rho)}(q)\delta(\hbar\omega - E_\alpha^{(\rho)}(q)) + \left(\Gamma^{(2)}|\mathbf{e}_{\rm I}\times\mathbf{e}_{\rm O}|\right)^2 \sum_{\alpha=1,2} C_\alpha^{(\sigma)}(q)\delta(\hbar\omega - E_\alpha^{(\sigma)}(q)) \right\}. \quad (67)$$

The intensities of the peaks are

$$C_\alpha^{(\nu)}(q) = \varepsilon_0 \left[w_{\alpha2}^{(\nu)}(q)\sqrt{1-Q} - w_{\alpha4}^{(\nu)}(q)\sqrt{1+Q}\right]^2. \quad (68)$$

The dependence of the peak intensities on the wave numbers of the interband CDE and SDE near resonance originating in the zero-order contribution are shown in Figure 6. The cross-over of the intensities is now observed to occur between the CDE. While at small q the CDE at $E_2^{(\rho)}$ has a high intensity, at higher q it is the CDE at $E_1^{(\rho)}$ which is stronger. In the depolarized configuration, the intensity of the energetically higher SDE at $E_2^{(\sigma)}$ is for all wave numbers much higher as compared to that at the lower energy.

The higher order contributions in (54) generate a large number of terms containing products of inter- and intra-subband operators (Appendix A). In lowest order, $n=1$, there are two terms, one proportional to $\kappa_\lambda(k,q)$, the second to $[\kappa_\lambda(k,q)]^2$. As an example, we give here the generalized density corresponding to the former.

$$N^{(1)}(q) = -\frac{\pi}{L}\sum_{i\neq j,\lambda}\sum_{q',l}\frac{\hbar^2}{m}\frac{k_{\rm F12}+\lambda q/2}{\left[\Delta_i+\lambda\hbar v_{\rm F12} q/2\right]^2} \times\{\Gamma^{(1)}\mathbf{e}_{\rm I}\cdot\mathbf{e}_{\rm O}\left[\rho_{ll}^{\lambda}(q-q')\rho_{ij}^{\lambda}(q') + \sigma_{ll}^{\lambda}(q-q')\sigma_{ij}^{\lambda}(q')\right] + {\rm i}\Gamma^{(2)}|\mathbf{e}_{\rm I}\times\mathbf{e}_{\rm O}|\left[\rho_{ll}^{\lambda}(q-q')\sigma_{ij}^{\lambda}(q') + \sigma_{ll}^{\lambda}(q-q')\rho_{ij}^{\lambda}(q')\right]\}. \quad (69)$$

This expression demonstrates explicitly the above general result, namely that inter-subband excitations are mixed with products of intra-subband modes. In the depolarized configuration, spin and charge modes are always mixed, due to the nature of the coupling of the photon field to the spin modes [21]. Whether or not the products of the charge and spin operators in the polarized configuration

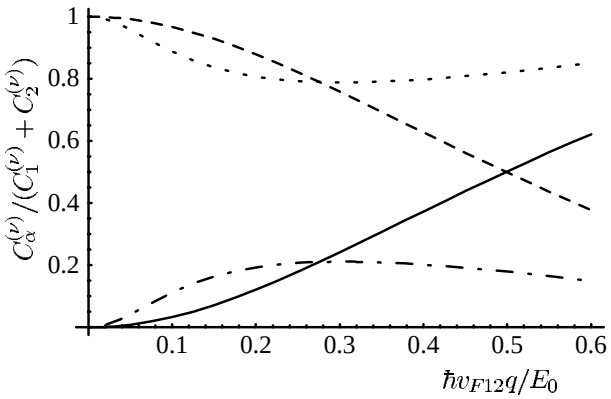

Fig. 6. Intensities of peaks $C_\alpha^{(\nu)}/(C_1^{(\nu)}+C_2^{(\nu)})$ near resonance as a function of the wave number q ($V = 1$, $V_{\rm ex} = 0.1$). Full line: $C_1^{(\rho)}$; dashed: $C_2^{(\rho)}$; dashed-dotted: $C_1^{(\sigma)}$; dotted: $C_2^{(\sigma)}$.

can lead to sharp peaks in the Raman spectra requires more detailed calculations [33]. Mainly, it depends on the form of the interband dispersion relations.

In order to find a peak in the Fourier transform of the density-density correlation function, the time evolution of the density should be dominated by a single frequency. In the above (69), this can be at best achieved for the spin-related term, $\propto \sigma_{ll}\sigma_{ij}$, in the polarized part. Since the dispersion of the interband spin excitations are practically linear in q, except for extremely small q (Fig. 3), the time evolution of the interband spin density operator can partially compensate the q'-contribution of the intraband spin density operator. Eventually, the time evolution will be determined only by the frequency of the interband SDE, thus giving rise for a peak at the corresponding energy. However, due to the deviations from the linear dispersion at very small wave number, this peak will be broadened, in contrast to the corresponding intra-subband SDE peak in the polarized configuration. From the products of the charge density operators, no sharp peaks are expected, due to the considerable deviations from linearity of the dispersions even at larger wave numbers (Fig. 3).

6 Comparison with experiment

The case of the intraband modes has been discussed earlier [20,21]. We concentrate on the interband excitations.

Quantum wires with two bands occupied have been investigated experimentally [9,10] in great detail. The observed intraband features are fully consistent with our predictions. An "interband CDE" is observed at energies $E(q)$ ($\approx$ 3 meV) which decreases slightly with the wave number. For $q \to 0$, its energy is about 10% larger than the (estimated) inter-subband spacing E_0. The polarization dependence of this excitation is not clearly reported. However, the mode seems to hybridize with the intraband CDE at a wave number of about one tenth of the Fermi wave number. A second mode is observed with a dispersion $E(q) \approx E(0) + \text{const} \cdot q$, with a positive constant. This has been assigned to an "interband-SPE". Near approximately $2E_0$, the presence of another broad peak with an energy almost independent of q has been reported, which was associated by the authors with an "inter-subband SPE" corresponding to transitions between the lowest and the second lowest subband.

From the parameters of the experiment [10] one concludes that the wave numbers that are experimentally accessible correspond in our model to the region $\hbar v_{\rm F12} q/E_0 \leq 0.5$ where the dispersion of the interband modes is only weak (Fig. 3). From the photon energies we conclude that the experimental spectra correspond to an intermediate region between extreme off-resonance (Fig. 4) and resonance (Fig. 5). Thus we expect that all interband modes described above contribute to the Raman spectra with more or less equal strengths.

In particular, we expect that the CDE- and SDE-modes in Figure 3 that decrease in energy with increasing q ($E_2^{(\rho)}$ and $E_1^{(\sigma)}$) cannot be clearly identified as SDE- or CDE-modes in experiment since they are energetically very close and would appear approximately as one and the same peak occurring in both polarizations. They can possibly be associated with the mode denoted as "inter-subband CDE" in reference [10] at about 3 meV. The hybridization with the intraband CDE cannot be reproduced by our model since we have assumed that inter- and intraband modes are completely decoupled. The "inter-subband SPE" of the experiment, with energy increasing with q, can be identified with a higher-order inter-subband SDE corresponding to the branch $E_2^{(\sigma)}$. The energetically highest mode $E_1^{(\rho)}$ has to be associated with the (depolarization-shifted) mode corresponding to the Raman peak near 6 meV.

As for the interaction matrix elements V and $V_{\rm ex}$ we obtain by comparison with the experimental data $V \approx 0.75$ and $V_{\rm ex} \approx 0.1\ V$. From the parameters of the experiment and by using the definitions (17, 18, 28) we find that $V_{12}/\lambda_{\rm F12} \approx E_{\rm F}$. This shows again that Coulomb interaction is important and cannot be neglected in etched quantum wires [23].

The experimental results obtained from quantum wires with more than two subbands occupied can also be considered to be consistent with the predictions of our bosonization model [13,14]. However, it has to be noted that in these experiments, the "interband CDE" mode with the energy decreasing with increasing q has not been observed. Also the depolarization shift of the symmetric interband CDE mode seems to be somewhat larger than in the two-band experiment.

7 Conclusion

We have presented a theory for the Raman spectra of electronic excitations in quantum wires with two subbands which is based on the bosonization method of the Tomonaga-Luttinger model. The excitation spectra have been found to be consistent with the available experimental data. The model allows to predict the Raman cross-section

as a function of parameters like temperature and photon energy.

We have provided an explanation of the "SPE"-modes which appear in the Raman spectra closer to resonance. These are identified as higher-order spin modes which do not obey the "classical selection rule".

In summary, the spin-charge separation predicted by the bosonization theory of 1D electrons is very clearly confirmed by the results of the Raman experiments.

However, additional experiments are necessary, in order to verify more clearly the predictions of our model. The Raman spectra of two-band quantum wires have to be re-investigated off- and in-resonance, in order to clarify especially the nature of the interband excitations. The dependence on the temperature of the intraband SPE-peaks has to be determined: we predict that their strengths increases with T [20,21] in contrast to the SDE modes which are independent of the temperature in our model. The dependence of the strengths of the intraband "SPE" peaks on the photon energy near resonance is predicted to be governed by a power law that contains the interaction [22], as is typical for the Luttinger liquid. Thus, a measurement of the behavior of the strengths of the intraband "SPE" peaks near resonance would help to clarify whether or not correlations between the electrons in a quantum wire show Luttinger liquid features.

The work is supported by EU (TMR-contracts FMRX-CT96-0042, FMRC-CT98-0180), by Istituto Nazionale di Fisica della Materia within PRA97 (QMTD), and by Deutsche Forschungsgemeinschaft within SFB 508 "Quantenmaterialien" and the Graduiertenkolleg "Nanostrukturierte Festkörper" of the Universität Hamburg.

Appendix A

We consider the operator

$$L^{\lambda,n}_{ij,s}(q)=\sum_k\left(k-\lambda k_{\mathrm{F}12}+\frac{q}{2}\right)^n c^{\lambda\dagger}_{is}(k+q)\,c^{\lambda}_{js}(k) \quad \text{(A.1)}$$

with $i\neq j$, (i and $j=1,2$, n integer and $k_{\mathrm{F}12}\equiv(k_{\mathrm{F}1}+k_{\mathrm{F}2})/2$. We have

$$L^{\lambda,n}_{ij,s}(q)=(\mathrm{i})^n\,\frac{\mathrm{d}^n}{\mathrm{d}\xi^n}\,I^{\lambda}_{ij,s}(q,\xi)\Big|_{\xi=0} \quad \text{(A.2)}$$

with

$$I^{\lambda}_{ij,s}(q,\xi)=\sum_k \mathrm{e}^{-\mathrm{i}(k-\lambda k_{\mathrm{F}12}+q/2)\xi}c^{\lambda\dagger}_{is}(k+q)c^{\lambda}_{js}(k). \quad \text{(A.3)}$$

This quantity can be written in terms of Boson fields [21]. By Fourier transforming the Fermion operators and replacing the sum over the wave number by an integral one finds

$$I^{\lambda}_{ij,s}(q,\xi)= \mathrm{e}^{\mathrm{i}\lambda k_{\mathrm{F}12}\xi}\int \mathrm{d}x\mathrm{e}^{\mathrm{i}qx}\psi^{\lambda\dagger}_{is}\left(x+\frac{\xi}{2}\right)\psi^{\lambda}_{js}\left(x-\frac{\xi}{2}\right). \quad \text{(A.4)}$$

Inserting the Boson representation of the Fermion fields in terms of the intra-subband densities

$$\psi^{\lambda}_{js}(x)=\sqrt{\frac{q_{\mathrm{c}}}{2\pi}}\mathrm{e}^{\mathrm{i}\lambda\left[k_{\mathrm{F}j}x-M^{\lambda}_{js}(x)\right]}, \quad \text{(A.5)}$$

with the operators

$$M^{\lambda}_{js}(x)=-\frac{2\pi\mathrm{i}}{L}\sum_q\frac{\mathrm{e}^{-\mathrm{i}qx}}{q}\rho^{\lambda}_{jj,s}(q), \quad \text{(A.6)}$$

and q_{c} is the cutoff wave number, one obtains

$$I^{\lambda}_{ij,s}(q,\xi)= \frac{q_{\mathrm{c}}}{2\pi}\int \mathrm{d}x\mathrm{e}^{\mathrm{i}qx}\mathrm{e}^{-\mathrm{i}\lambda(k_{\mathrm{F}i}-k_{\mathrm{F}j})x}\mathrm{e}^{\mathrm{i}\lambda\left[M^{\lambda}_{is}(x+\xi/2)-M^{\lambda}_{js}(x-\xi/2)\right]}. \quad \text{(A.7)}$$

Considering in (A.1) only the term with $n=1$ we have

$$L^{\lambda,1}_{ij,s}(q)=\frac{\pi\lambda}{L}\sum_{q'}\sum_{l=1,2}\rho^{\lambda}_{ll,s}(q-q')\rho^{\lambda}_{ij,s}(q')\,. \quad \text{(A.8)}$$

Appendix B

The solutions of equation (33) are pairs of branches of positive and negative eigenvalues and correspond by construction to $q>0$, and to four non-bosonic eigenmodes. These can be transformed into the two branches of positive eigenvalues of H_ν which correspond to $-\infty<q<\infty$. This is achieved by suitably mapping the four independent γ-operators into two boson operators.

Consistently with equations (34, 35) we replace

$$\gamma^{(\nu)}_{\alpha}(q)\to\begin{cases}\gamma^{(\nu)}_{\alpha}(q), & \omega^{(\nu)}_{\alpha}(q)>0\\ \gamma^{(\nu)\dagger}_{\alpha}(-q), & \omega^{(\nu)}_{\alpha}(q)<0\end{cases} \quad \text{(B.1)}$$

$$\omega^{(\nu)}_{\alpha}(q)=\begin{cases}E^{(\nu)}_{\alpha}(q), & \omega^{(\nu)}_{\alpha}(q)>0\\ -E^{(\nu)}_{\alpha}(-q), & \omega^{(\nu)}_{\alpha}(q)<0\end{cases} \quad \text{(B.2)}$$

with the new γ satisfying

$$\left[\gamma^{(\nu)}_{\alpha}(q),\gamma^{(\nu')\dagger}_{\alpha'}(q')\right]=\delta_{\nu\nu'}\delta_{qq'}\delta_{\alpha\alpha'} \quad \text{(B.3)}$$

and all other commutators vanishing.

By inserting into (37) we obtain, apart from an additive constant

$$H_\nu=\sum_{\alpha=1,2}\sum_q E^{(\nu)}_{\alpha}(q)\gamma^{(\nu)\dagger}_{\alpha}(q)\gamma^{(\nu)}_{\alpha}(q). \quad \text{(B.4)}$$

The eigenenergies are

$$E^{(\rho)}_{\alpha}(q;V)=E_0\left\{1+2V\ +Q^2\left[1+2V +2V_{\mathrm{ex}}(2V-V_{\mathrm{ex}})\right]-(-1)^{\alpha}\Delta\right\}^{1/2} \quad \text{(B.5)}$$

with the abbreviations

$$\begin{aligned}
\Delta &\equiv \left[4(V-V_{\rm ex})^2 + A_2 Q^2 + A_4 Q^4\right]^{1/2}, \\
A_2 &\equiv 4\left[1 + 4V + 2V^2 \right. \\
&\quad \left. + V_{\rm ex}(6V + 4V^2 - 3V_{\rm ex} - 2VV_{\rm ex})\right], \\
A_4 &\equiv 4\left[V^2 + V_{\rm ex} \right. \\
&\quad \left. \times (4V^2 - 2VV_{\rm ex} + 4V^2 V_{\rm ex} - 4VV_{\rm ex}^2 + V_{\rm ex}^3)\right].
\end{aligned}$$

The SDE energies are given by

$$E_\alpha^{(\sigma)}(q) = E_\alpha^{(\rho)}(q; V=0). \tag{B.6}$$

The first components of the eigenvectors are

$$\begin{aligned}
\left[w_{\alpha 1}^{(\nu)}\right]^2 = {\rm sgn}(\omega_\alpha^{(\nu)}) \Bigg\{ 1 - \left(K_\alpha^{(\nu)} \frac{\omega_\alpha^{(\nu)} - \omega_0^+}{\omega_\alpha^{(\nu)} + \omega_0^-} \right)^2 \\
+ \left(\frac{b_+}{c}\right)^2 \left[\left(K_\alpha^{(\nu)}\right)^2 - \left(\frac{\omega_\alpha^{(\nu)} - \omega_0^-}{\omega_\alpha^{(\nu)} + \omega_0^+} \right)^2 \right] \Bigg\}^{-1}
\end{aligned} \tag{B.7}$$

where, using the definitions (27)

$$\begin{aligned}
K_\alpha^{(\nu)} = \left(b_- - b_+ \frac{\omega_\alpha^{(\nu)} - \omega_0^-}{\omega_\alpha^{(\nu)} + \omega_0^+} \right) \\
\times \frac{\omega_\alpha^{(\nu)} + \omega_0^-}{(\omega_\alpha^{(\nu)} + E_0 h_-)(\omega_\alpha^{(\nu)} - \omega_0^+) - (\omega_\alpha^{(\nu)} + \omega_0^-) d b_+ / c}
\end{aligned} \tag{B.8}$$

with $\omega_0^\pm = E_0(1 \pm Q)/\hbar$. The other components can be determined from the relations given in 4.3.

References

1. *Mesoscopic Quantum Physics*, edited by E. Akkermans, G. Montambaux, J.-L. Pichard, J. Zinn-Justin (Elsevier Science, Amsterdam, 1995).
2. *Quantum Dynamics of Submicron Structures*, edited by H.A. Cerdeira, B. Kramer, G. Schön, NATO ASI Ser. E **291** (Kluwer Academic Publishers, Dordrecht, 1995).
3. F.A. Blum, Phys. Rev. B **1**, 1125 (1970).
4. D.C. Hamilton, A.L. McWhorter, in *Light Scattering Spectra of Solids*, edited by G.B. Wright (Springer Verlag, New York, 1969), p. 309.
5. M.V. Klein, in *Light Scattering in Solids*, Topics Appl. Phys. **8**, edited by M. Cardona (Springer Verlag, Heidelberg, 1975), p. 147.
6. A. Pinczuk, E. Burstein, in *Light Scattering in Solids*, Topics Appl. Phys. **8**, edited by M. Cardona (Springer Verlag, Heidelberg, 1975), p. 23.
7. G. Abstreiter, R. Merlin, A. Pinczuk, J. Quantum Electronics **QE-22**, 1771 (1986).
8. A. Pinczuk, G. Abstreiter, in *Light Scattering in Solids V*, Topics Appl. Phys. **66**, edited by M. Cardona, G. Güntherodt (Springer Verlag, Heidelberg, 1988), p. 153.
9. A.R. Goñi *et al.*, Phys. Rev. Lett. **67**, 3298 (1991).
10. A.R. Goñi *et al.*, in *Phonons in Semiconductor Nanostructures*, edited by J.P. Leburton, J. Pascual, C.S. Torres (Plenum, New York, 1993), p. 287.
11. A. Schmeller *et al.*, Phys. Rev. B **49**, 14778 (1994).
12. R. Strenz *et al.*, Phys. Rev. Lett. **73**, 3022 (1994).
13. C. Schüller *et al.*, Phys. Rev. B **54**, R17304 (1996).
14. G. Biese, Ph.D Thesis, Universität Hamburg, 1996.
15. H.J. Schulz, Phys. Rev. Lett. **71**, 1864 (1993).
16. Ben Yu-Kuang Hu, S. Das Sarma, Phys. Rev. B **48**, 5469 (1993).
17. J.M. Luttinger, J. Math. Phys. **4**, 1154 (1963).
18. F.D.M. Haldane, J. Phys. C **14**, 2585 (1981).
19. J. Voit, Rep. Progr. Phys. **57**, 977 (1995).
20. M. Sassetti, B. Kramer, Phys. Rev. Lett. **80**, 1485 (1998).
21. M. Sassetti, B. Kramer, Eur. Phys. J. B **4**, 357 (1998).
22. M. Sassetti, B. Kramer, Ann. Phys. **7**, 508 (1998).
23. M. Sassetti *et al.*, in *The Physics of semiconductors*, edited by D. Gershoni (World Scientific, Singapore, 1999).
24. M. Sassetti, F. Napoli, B. Kramer, Phys. Rev. B **59**, 7297 (1999).
25. E.H. Hwang, S. Das Sarma, Phys. Rev. B **50**, 17267 (1994).
26. A. Brataas *et al.*, J. Phys.-Cond. **8**, L325 (1996).
27. A. Brataas *et al.*, Phys. Rev. B **55**, 13161 (1997).
28. A.L. Fetter, J.D. Walecka, *Quantum Theory of Many Particle Systems* (McGraw-Hill, New York, 1971).
29. A.M. Finkel'stein, A.I. Larkin, Phys. Rev. B **47**, 10461 (1993).
30. M. Fabrizio, Phys. Rev. B **48**, 15838 (1993).
31. H.J. Schulz, Phys. Rev. B **53**, R2959 (1996).
32. K. Penc, J. Solyom, Phys. Rev. B **47**, 6273 (1993).
33. E. Mariani, M. Sassetti, B. Kramer (unpublished, 1999).